Elasto—Plastic Constitutive Model for Compacted Silt—Fly Ash Admixture

by

K. G. Sharma*

G. Venkatappa Rao**

J. C. Sharma***

Introduction

The importance of constitutive laws of geologic media for appropriate numerical prediction is now well recognized. There are two distinct categories of non-linear constitutive models. In the first category are the non-linear elasticity models in which an attempt is made to simulate the stress-strain curve upto the failure by a set of mathematical functions such as hyperbola and spline functions (Duncan and Chang, 1970 ; Naylor, 1975 ; Desai, 1971). In the second category are the models of elasto/plasticity with different yield criteria (Zienkiewicz and Cormeau, 1974 ; Lade and Duncan, 1975 ; Drucker et al.. 1957). Cap models proposed by Roscoe and Burland (1968) and Di Maggio and Sandler (1971) are of the second category. In the present paper, an elasto/plastic constitutive model (second category) is developed based on laboratory tests on silt-fly ash admixture under repeated loads.

Elasto/Plastic Behaviour

Simple linear elastic models have been often used to analyse the soil behaviour but stress-stain response of the soil from laboratory tests indicate non-linearity from the beginning of the loading. Unloading of the soil sample results inpermanent strain (plastic strain). Therefore, elasto/plastic model was adopted to represent the soil behaviour.

The strain increment $d\epsilon_{ij}$ due to a stress increment $d\sigma_{ij}$ consists of elastic ($d\epsilon_{ij}^{e}$) and plastic ($d\epsilon_{ij}^{p}$) components.

$$d\epsilon = d\epsilon_{ij}^{e} + d\epsilon_{ij}^{p} \qquad ...(1)$$

The incremental plastic strain is given by the flow rule

$$d\epsilon_{ij}^{p} = \Phi \frac{\partial F}{\partial \sigma_{ij}} \qquad ...(2)$$

* Assistant Professor
** Principal Scientific Officer
*** Part time Graduate Student

Civil Engineering Department, Indian Institute of Technology, Delhi, New Delhi-110016, INDIA.

(*This paper was received in October 1983 and is open for discussion till the end of June 1984.*)

where Φ is a proportionality constant and F is the yield function. The rule given by Equation (2) is known as the normality principle because the plastic strain increment is normal to the yield surface F and the material is said to follow the associated flow rule. If the plastic potential Q and the yield function F are different, then the flow rule will be

$$d\epsilon_{ij}^{p} = \Phi \frac{\partial Q}{\partial \sigma_{ij}} \quad \ldots(3)$$

and then non-associated flow rule results.

For the present study, the elasto/plastic model consists of a failure envelope (or surface) and a yield surface (cap) and associated flow rule (Equation 2) has been assumed. The methodology for evaluating the failure and yield surfaces is described in the paper and also the hardening/softening behaviour of the cap is discussed. In total ten parameters (4 for failure surface and 6 for the cap) are needed to describe the model. The model has been used to predict the stress-strain behaviour under various stress paths.

Material Tested

Delhi Silt (per cent sand = 42, per cent silt = 46, per cent clay = 12, L.L. (per cent) = 27, P.I. (per cent) = 9) is used in this investigation. The fly ash used as an additive was procured from Indraprastha Thermal Power Station, Delhi, which has 57 per cent silica and 28 per cent Alumina. An admixture of silt and fly ash (3 : 1) is used in the present study. Under standard Proctor compaction conditions (light compaction), the optimum moisture content is 17.0 per cent and maximum dry density is 1.44g/cc.

The Apparatus

The Universal Triaxial Apparatus (UTA—Type II) developed by Ramamurthy et al (1979) is used for the study. The major features of this apparatus are also described in Venkatappa Rao et al (1983). It consists of three major components viz. (*a*) rigid self-straining square frame to provide support for lateral pressure application, (*b*) the lateral loading device, consisting of two pairs of identical hydraulic jacks and a self-compensating mercury pot system (*c*) the loading machine (INSTRON—1195) capable of applying static and cyclic loads in vertical direction. A plan and elevation of this apparatus are shown in Figs. 1a and b. 76mm cuboidal specimens can be tested in this apparatus under desired stress paths, as the principal stresses can be varied independently and the corresponding strains measured. The specimens are compacted statically at Proctor optimum condition.

Triaxial Tests

Triaxial tests are conducted along various stress paths at different mean stress levels to obtain stress-strain properties of the soil and also the failure stress level. The stress paths are shown in Fig. 2, where p is the mean stress $(\sigma_1+\sigma_2+\sigma_3)/3$ and q is the deviatoric stress $(\sigma_1-\sigma_3)$. In the figure, *HC* represents hydrostatic compression ; *TC* and *TE*, triaxial compression and extension ; *TPSC* and *TPSE*, triaxial pure shear compression and extension (mean stress p is kept constant).

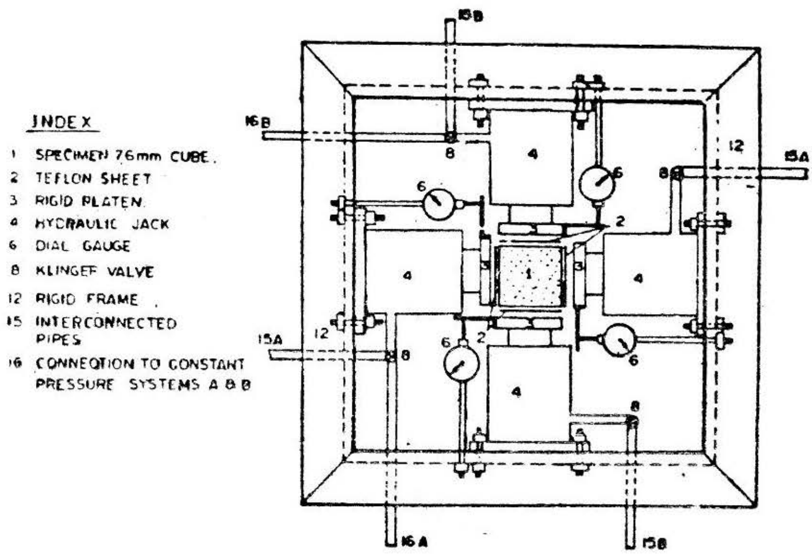

FIGURE 1a Schematic Plan of Universal Triaxial Apparatus—II

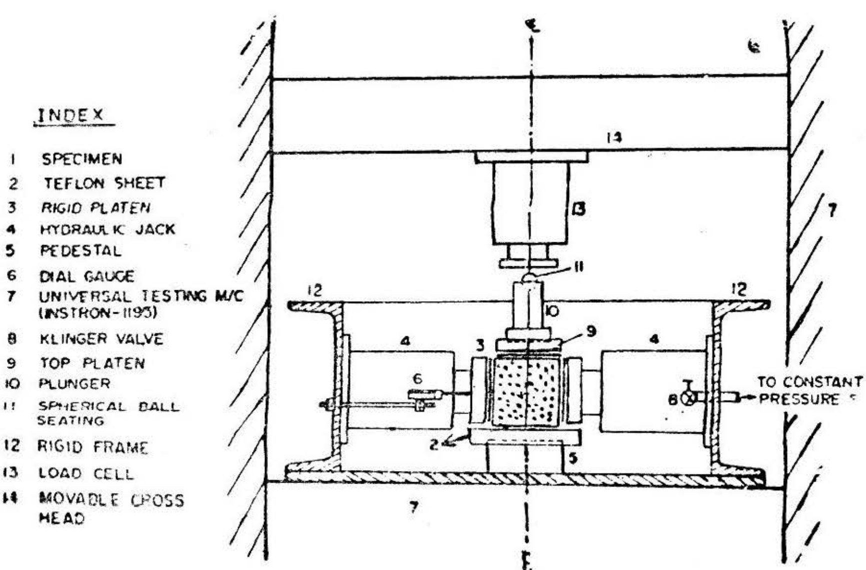

FIGURE 1b Sectional Elevation of Universal Triaxial Apparatus—II, Placed in INSTRON—1195, UTM.

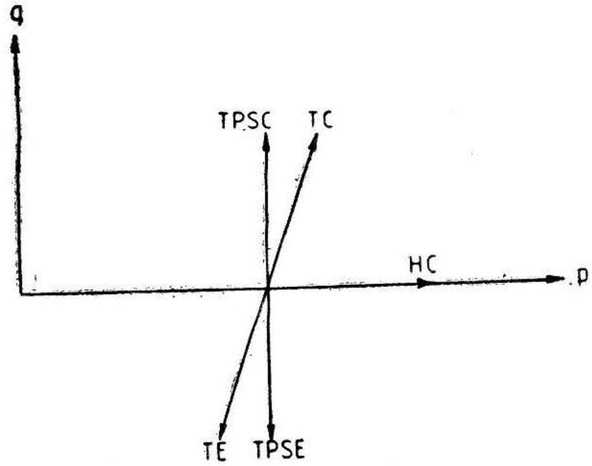

FIGURE 2 Stress Paths in $q-p$ Space

Typical test results along hydrostatic compression stress path (*HC*) are shown in Fig. 3 for initial consolidation pressure p_i of 0.83 Kg/cm^2. The test results along triaxial compression stress path (*TC*) are plotted in Fig 4 for initial consolidation pressure p_i of 3.3 Kg/cm^2. Several tests were conducted along different stress paths and it was found that the stress-strain—strength behaviour of the soil were function of the mean stress p and deviatoric stress q. This has also been reported by Sture et al (1979).

Development of Constitutive Model

Elastic Parameters

From the cyclic hydrostatic compression tests, volumetric strain ϵ_v was plotted against mean stress p (on logarithmic scale) for loading and unloading as shown in Fig. 5. Both loading and unloading curves are straight lines. Slope of loding curve gives compression index λ and that of unloading curve gives swelling index k. For the present soil, $\lambda = 0.0268$ and $k = 0.00345$. Then the bulk modulus, K is given by

$$K = \frac{p}{k} \qquad \text{...(4)}$$

which varies with the mean stress. For determining shear modulus, G, shear stress versus shear stain slope of unloading curve of pure shear compression test was used. The value was found to be 3751 Kg/cm^2.

Failure Surface

Fig. 6 shows the failure surface in $q-p$ space for various tests conducted in the laboratory. In this figure, for each stress path, the failure stress has been plotted and the curve joining all such points gives the failure envelope or failure surface. As can be seen from Fig. 6, the failure surface consists of straight line portion (Drucker—Prager failure

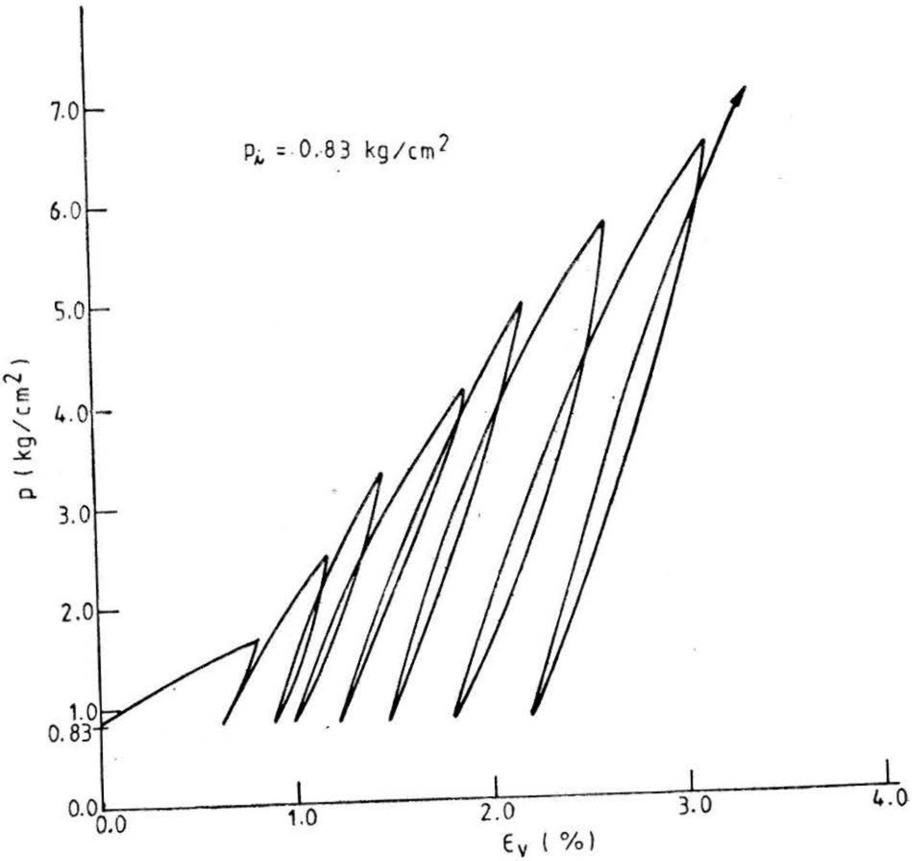

FIGURE 3 Mean Stress Versus Volumetric Strain Curve for Cyclic Hydrostatic Compression.

surface) for $p \geqslant 5.9$ Kg/cm^2 and an exponential transition surface for $p \leqslant 5.9$ Kg/cm.^{2} Following expression has been used to represent the failure surface.

$$q = a + bp - ce^{-\theta p} \qquad \ldots(5)$$

where a, b, c, θ are constants.

The slope of the straight line (Fig. 6) gives the constant b, which in the present case comes out to be 1.5556. The straight line when extended back gives intercept on q—axis as 'a'. From Figure 6, 'a' is 3.0. Since the failure envelope starts from the origin, therefore, $a - c = 0$. Thus $c = a = 3.0$. By taking any point on the curve, the remaining constant θ is worked out, which is calculated as 0.6. Thus.

$$F_1 = q - 3.0 - 1.5556\, p + 3.0\, e^{-0.6p} = 0 \qquad \ldots(6)$$

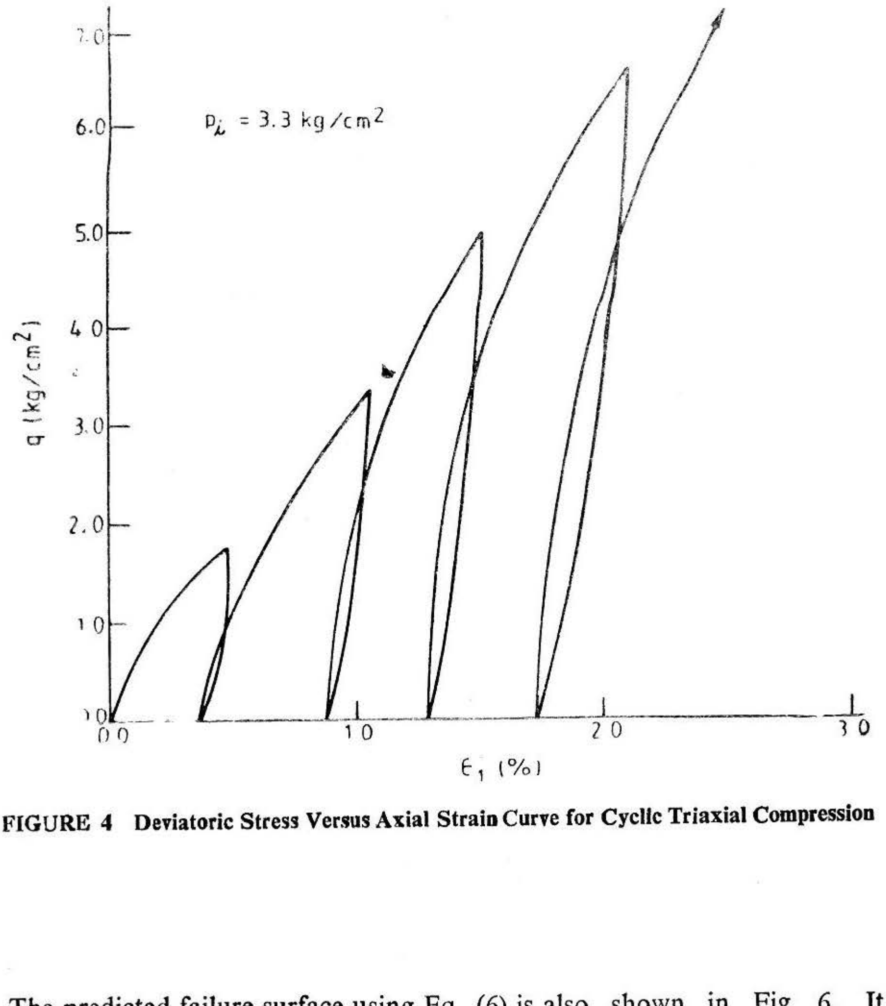

FIGURE 4 Deviatoric Stress Versus Axial Strain Curve for Cyclic Triaxial Compression

The predicted failure surface using Eq. (6) is also shown in Fig. 6. It is seen that Eq. (6) represents the failure surface accurately.

Hardening/Softening Cap

To obtain the shape of the moving cap, the accumulated volumetric plastic strain, ϵ_v^p, is computed at selected points along the stress paths and volumetric plastic strain contours (ϵ_v^p is constant on the contour) are drawn as shown in Fig. 7. As can be seen, the shape of the cap resembles an ellipse. Therefore, the shape will be represented by the ellipse as

$$F_2 = F_2 (p, q, \epsilon_v^p).$$

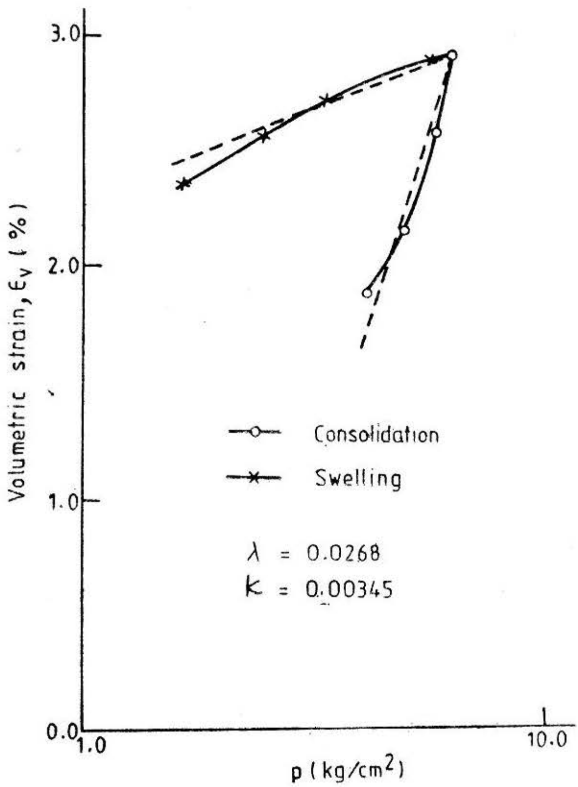

FIGURE 5 Compression and Swelling Curves due to Hydrostatic Compression

Fig. 8 shows the failure envelope F_1 with an elliptical cap F_2. The equation of surface F_2 can be written as

$$F_2 = \frac{q^2}{B^2} + \frac{(p-C)^2}{p_c^2} - 1 = 0 \qquad ...(6)$$

where C = p value at the centre of the ellipse,

B = half of the minor axis intercept i.e. q value at $p = C$, and

p_c = half of the major axis intercept,

By substituting $p = C$ in Equation (6), B can be determined.

The p value at the centre of the ellipse is related to the volumetric plastic strain by the expression

$$C = C_0 (1 + \alpha \, \epsilon_v^p)^\beta \qquad ...(8)$$

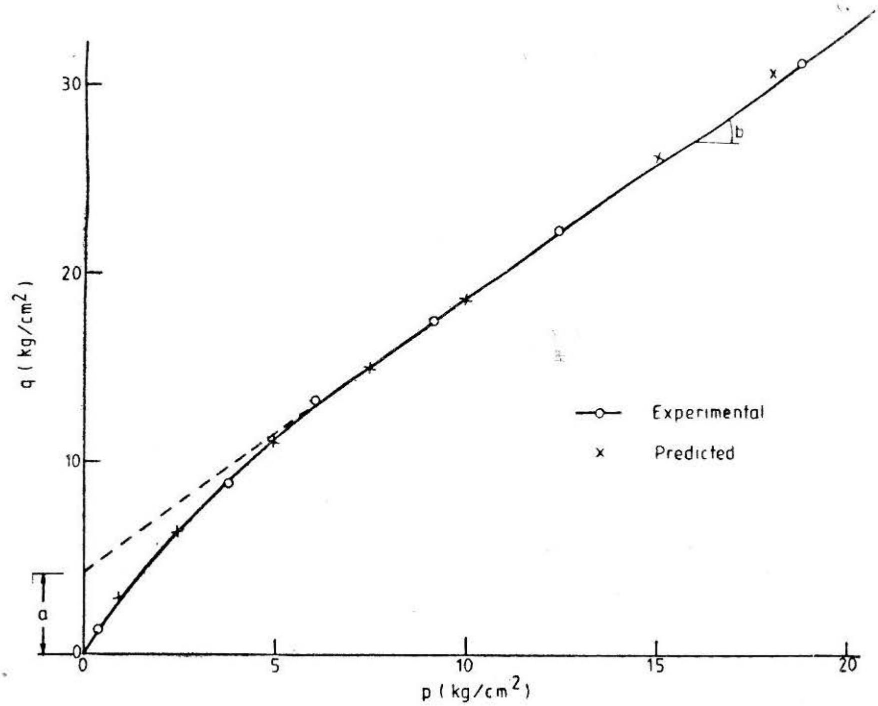

FIGURE 6 Failure Surface in $q-p$ Space

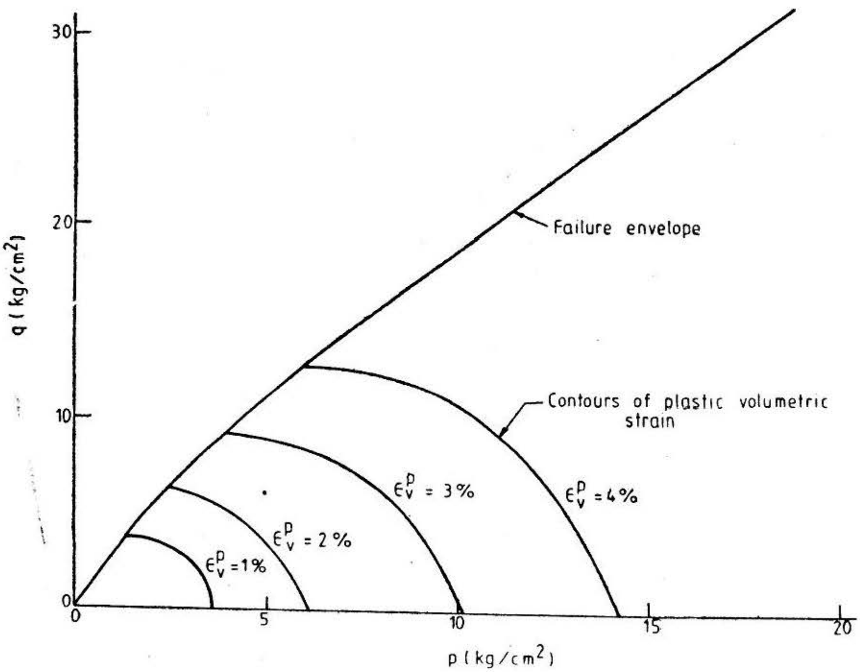

FIGURE 7 Yield Surfaces (ucaps) in $q-p$ Space

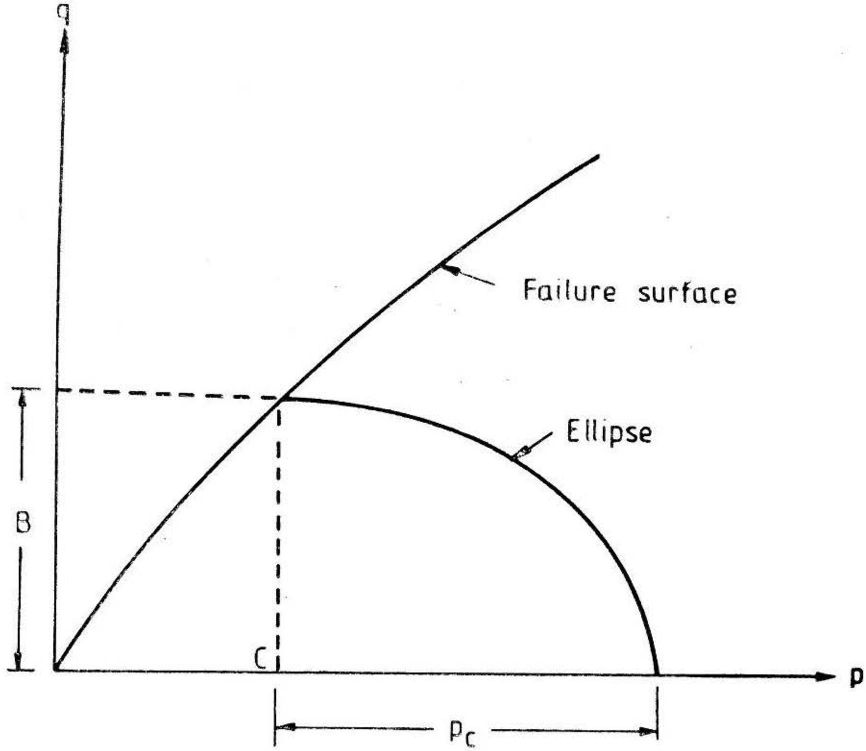

FIGURE 8 Typical Elliptical Yield Surface with a Failure Surface

For the results plotted in Figure 7, using regression analysis, we obtain

$$C_o = 0.542,\ \alpha = 50.0,\ \beta = 2.1575.$$

In any test, as the stress is increased, the cap will harden which means the ellipse will increase in size as well as the cap will move (Equation (8)). The hardening behaviour of the cap is representedd by

$$p_c = p_{c0}\ e^{x\epsilon_v^p} \qquad \text{...(9)}$$

where p_{co} and x are constants. As proposed by Roscoe and Burland (1968), the hardening factor x is given by

$$x = \frac{1}{\lambda - k} \qquad \text{...(10)}$$

From the values of λ and k given in the earlier sections, $x = 42.81$. From the results of Figure 7, p_{co} is calculated as 1.5 Kg/cm^2.

Equations (6) to (10) represent a cap model with ten parameters (a, b, c, θ, α, β, λ, k, C_o, p_{co}).

Prediction of Stress-Strain Behaviour

For predicting the stress-strain behaviour, associated flow rule given by Equation (2) was used along with Equations (6) to (10). To obtain elastic strains, two elastic constants K (Eq. (4)) and G (4751 kg/cm^2) were used.

Test results corresponding to hydrostatic compression stress path are shown Fig 9 for initial mean stress of p_i = 0.83 kg/cm^2. The predicted results are also plotted in the same figure. It is seen that the constitutive model predicts the behaviour well.

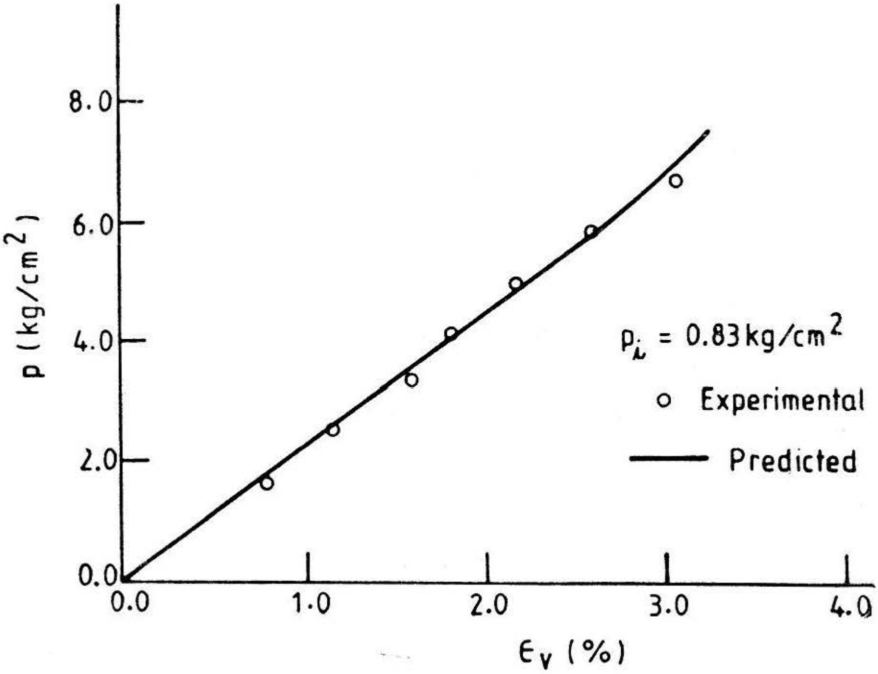

FIGURE 9 Stress-Strain Curve for Monotonic Hydrostatic Compression

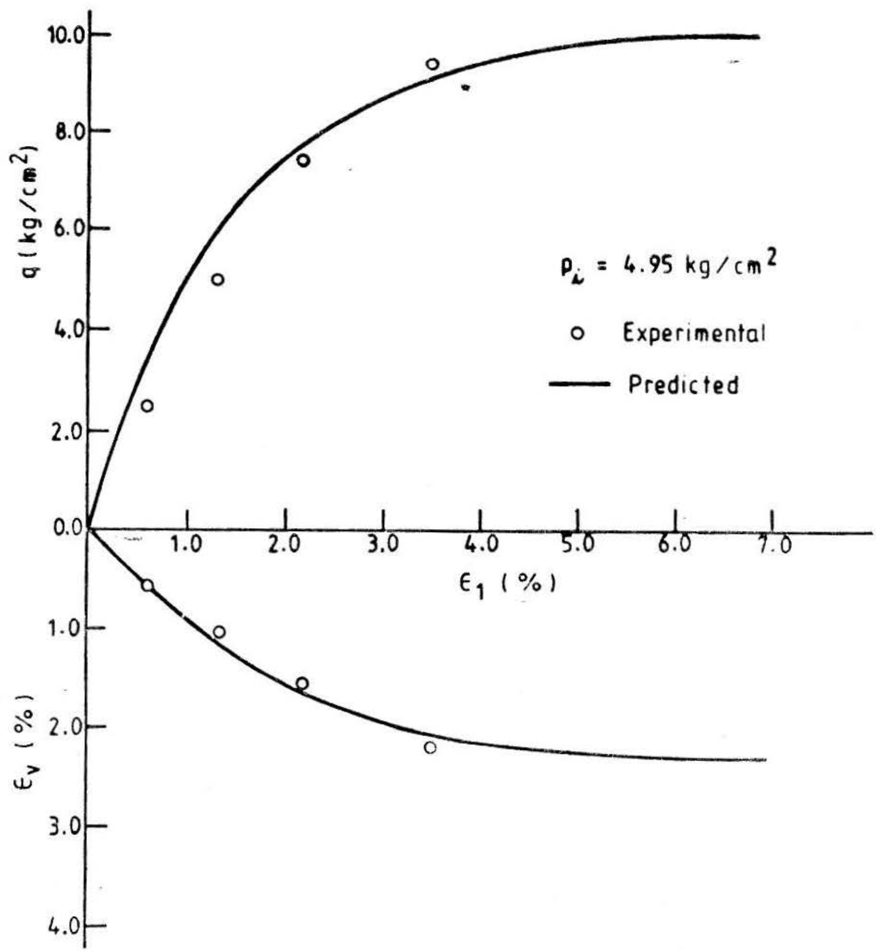

FIGURE 10 Stress-Strain Curves for Monotonic Triaxial Pure Shear Compression

In Fig. 10 are plotted the experimental and predicted results for p-constant (4.95 kg/cm^2) stress path. The matching of both the results is satisfactory.

For the triaxial compression (TC) with initial consolidation pressure p_i of 3.3 kg/cm^2, observed and predicted results are shown in Figure 11. Both the results compare well as is seen from Fig. 11.

The matching may be closer if non-associated flow rule is used but this requires derivation of the plastic potential, Q. This work is in progress.

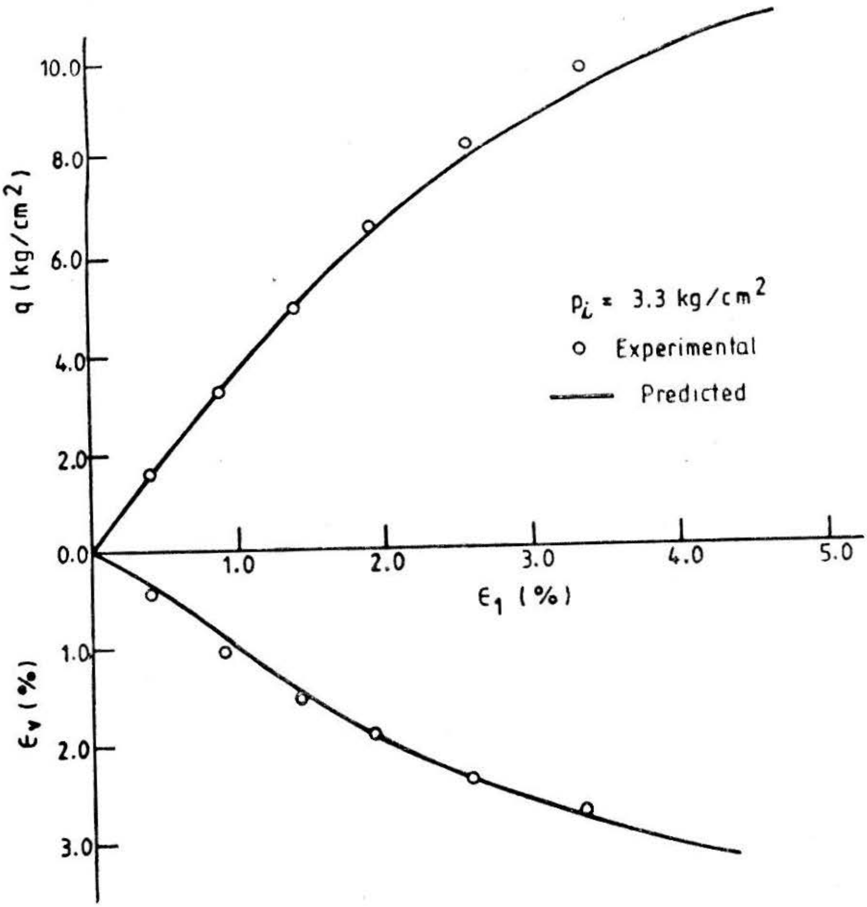

FIGURG 11 Stress-Strain Curves for Monotonic Triaxial Compression

Conclusions

A ten parameter elasto/plastic constitutive model for silt-fly ash admixture has been presented in this paper. The model takes into consideration different stress paths and stress path dependent strain hardening behaviour of the soil. The predicted results match well with experimental results.

References

DESAI, C.S. (1971), "Non-linear Analysis using Spline Function", *JSMFE, ASCE*, 97: SM: 1461-1480.

DI MAGGIO, F.L., and SANDLER, I.S. (1971), "Material Model for Granular Soils", *JEM, ASCE*, 97 : 3 : 935-950.

DRUCKER, D.C., GIBSON, R.E. and HENKEL, D.J., (1957), "Soil Mechanics and Work-hardening Theories of Plasticity", *Trans ASCE*, 122 : 338-346.

DUNCAN, J.M. and CHANG, C.Y. (1970), "Non-linear Analysis of Stress and Strain in Soil", *JSMFE, ASCE*, 96: SM5: 1629-1653.

LADE, P.V. and DUNCAN, J.M. (1975), "Elasto-plastic Stress-Strain Theory for Cohesionless Soils", *J. Geotech. Engg. Div., ASCE,* 101: GT 10: 1037-1053.

NAYLOR, D.J. (1975), "*Non-linear Finite Element Models for Soils*", Ph.D. thesis submitted to University of Wales, Swansea.

RAMAMURTHY, T., VENKATAPPA RAO, G. and NAG, C.P. (1979), "Development of Universal Triaxial Test Apparatus for Evaluation of Pavement Material Characteristics" *International Symposium on Pavement Evaluation and Overlay Design,* Rio-de-Jeneiro, Brazil.

ROSCOE, K.H. and BURLAND, J.B. (1968), "On the Generalized Stress-Strain behaviour of 'Wet' clays", In *Engineering Plasticity* (Ed. J. Heyman and F.A. Lackie), Cambridge University Press, pp 505-609.

SCHOFIELD, A. and WROTH, C.P. (1968), "*Critical State Soil Mechanics*", Mc Graw-Hill, London.

STURE S., DESAI, C.S. and JANARDHANAM, R. (1979), "Development of a Constitutive Law for an Artificial Soil", *Proc. 3rd Int. Conf. on Numerical Methods in Geomech.,* Aachen, 1: 309-317.

VENKATAPPA RAO, G., RAMAMURTHY, T. and NAG, C.P. (1983), "Soil Cement response to Cyclic Loading in General Stresses", *Proc. Indian Geotechnical Conference-83,* Madras, I : III-7 to III-12.

ZIENKIEWICZ, O.C. and CORMEAU, I.C. (1974), "Visco-plasticity, Plasticity and Creep in Elastic Solids. A Unified Numerical Solution Approach" *Int. J. Num. Methods Engg.,* 8: 821-845.

Notation

B	Half of minor axis intercept of ellipse
C	Mean stress at the centre of ellipse
F	Yield Surface
F_1	Failure surface
F_2	Yield Surface (Cap)
G	Shear modulus
K	Bulk modulus
p	Mean stress
p_c	Half of major axis intercept of ellipse
p_i	Initial isotropic consolidation pressure
q	Deviatoric stress
Q	Plastic potential surface
a, b, c, C_o, p_{co}	Constants
α, β, θ	Constants
ϵ_1	Axial Strain
ϵ_v	Volumetric strain

ϵ_v^p	Plastic volumetric strain
$d\epsilon_{ij}$	Incremental strain (Indicial notation)
$d\epsilon_{ij}^e$	Incremental elastic strain (Indicial notation)
$d\epsilon_{ij}^p$	Incremental plastic strain (Indicial notation)
k	Swelling index
x	Hardening factor
λ	Compression index
Φ	Proportionality constant
$\sigma_1, \sigma_2, \sigma_3$	Principal stresses
σ_{ij}	Stresses (Indicial notation)